Supplementary figures

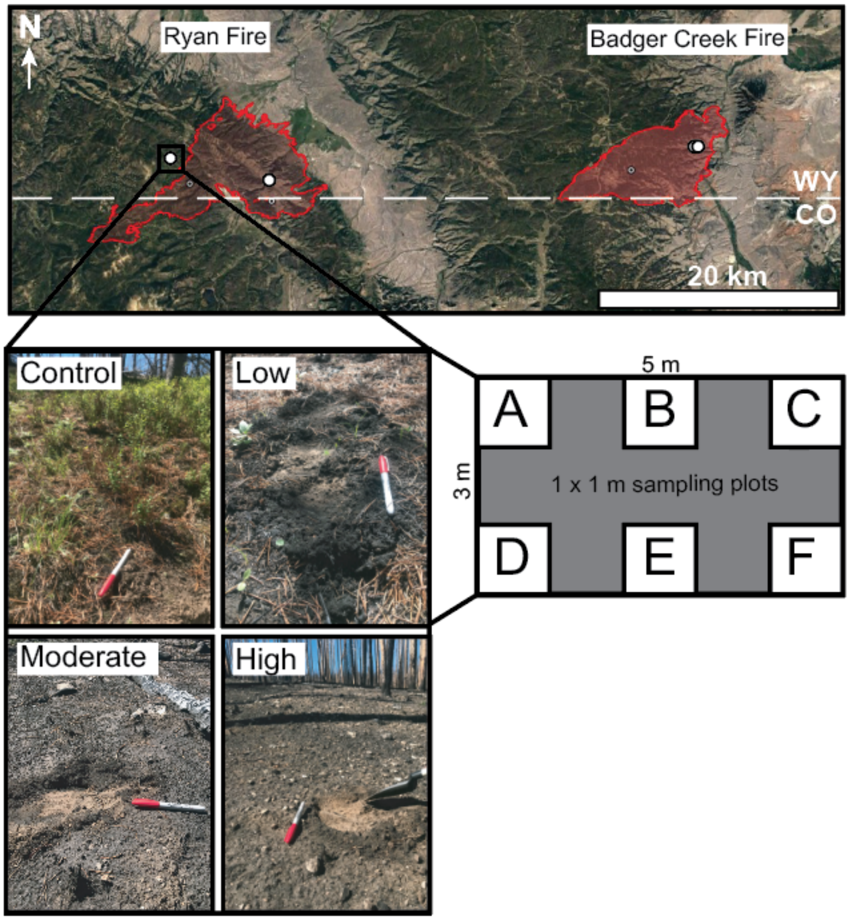

Figure S1. Schematic of sampling design. There were four replicate burn severity gradients (two at Ryan Fire and two at Badger Creek Fire); six subsamples were collected in each burn condition at each gradient. Burn severity classes were based on Parson et al. (2010).

Sample	TMM high expression cutoff
R85	1.68
R86	3.26
R89	1.47
R90	3.16
R93	1.68
R94	3.28
R109	1.68
R110	2.24
R113	1.68
R114	2.11
R117	1.61
R118	1.87

Table S1. TMM cutoff values for high expression analysis in each sample. Values correspond to the 20th percentile value TMM. Transcripts were highly expressed if the TMM was above this value for 2/3 samples in any one condition.

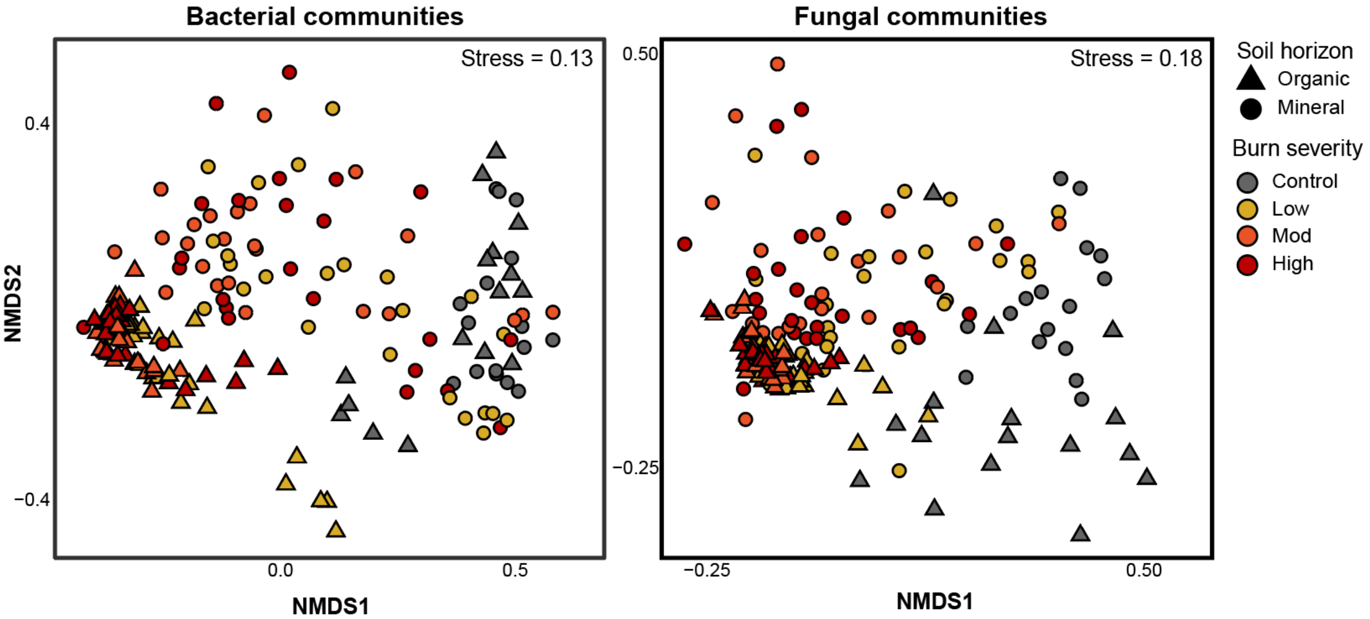

Figure S2. Non-metric multidimensional scaling (NMDS) ordination of all bacterial (left) and fungal (right) communities shaped by soil horizon and colored by burn severity.

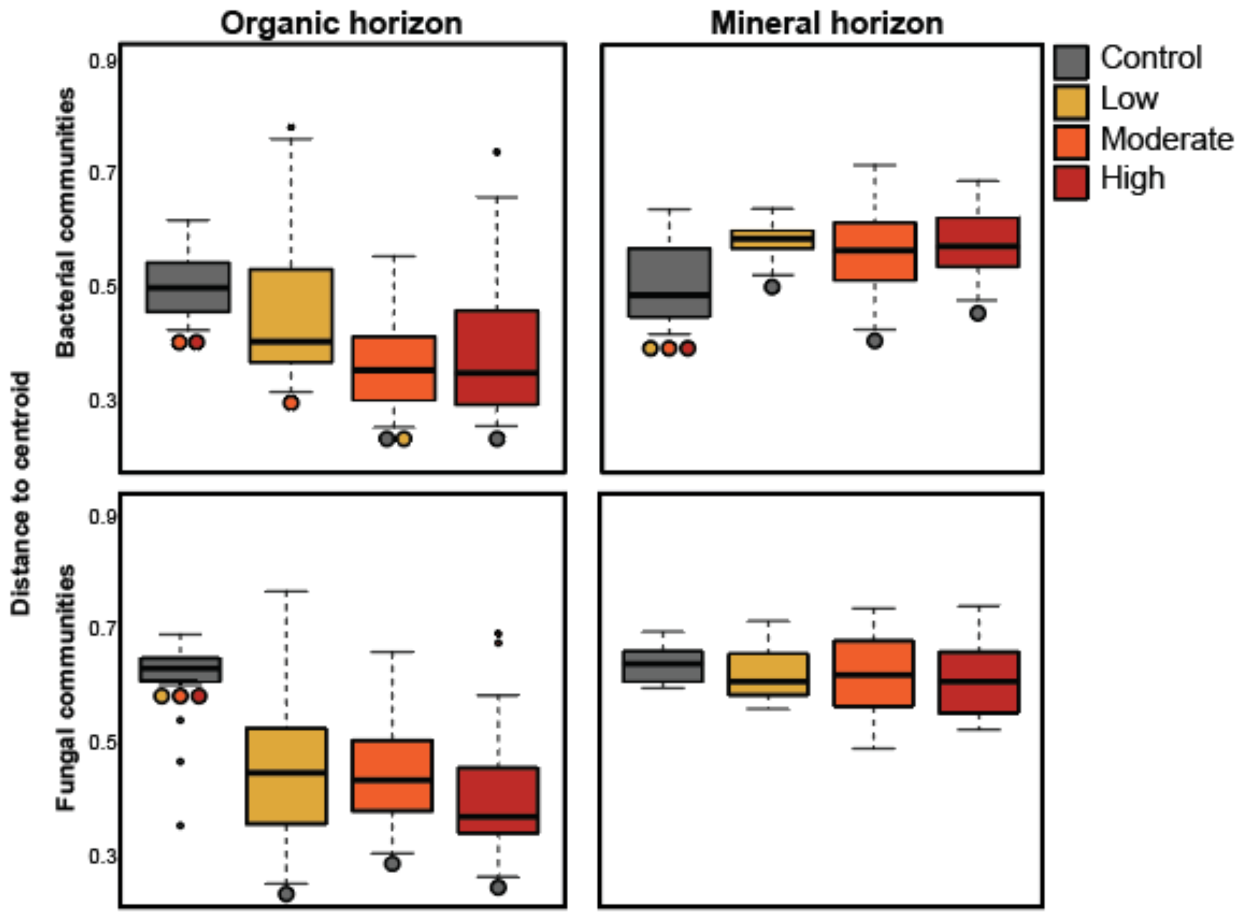

Figure S3. Distance to centroid calculations of the NMDS ordinations or O-horizon and A-horizon bacterial (top) and fungal (bottom) communities by burn severity. Colored points indicate significant differences ($p<0.05$) between conditions.

Condition	Nodes	Edges	Edge:node	Modules	N samples
Bacterial communities					
Control, organic	10426	3662534	351.3	16	16
Low, organic	6234	1194870	191.7	22	24
Moderate, organic	2442	196930	80.6	11	24
High, organic	2193	277073	126.3	11	24
Control, mineral	9452	2769191	292.9	16	16
Low, mineral	9132	1904471	208.5	21	24
Moderate, mineral	5916	1376628	232.7	18	24
High, mineral	6415	1151930	179.6	19	24
Fungal communities					
Control, organic	2491	271323	108.9	12	16
Low, organic	1548	126698	81.8	11	24
Moderate, organic	238	14366	60.3	2	24
High, organic	260	17026	65.5	2	24
Control, mineral	1569	145649	92.8	9	16
Low, mineral	681	48389	71.1	5	24
Moderate, mineral	242	14558	60.1	3	24
High, mineral	374	23626	63.1	3	24

Table S2. Characteristics of WGCNA networks created from 16S rRNA gene sequencing data from each condition.

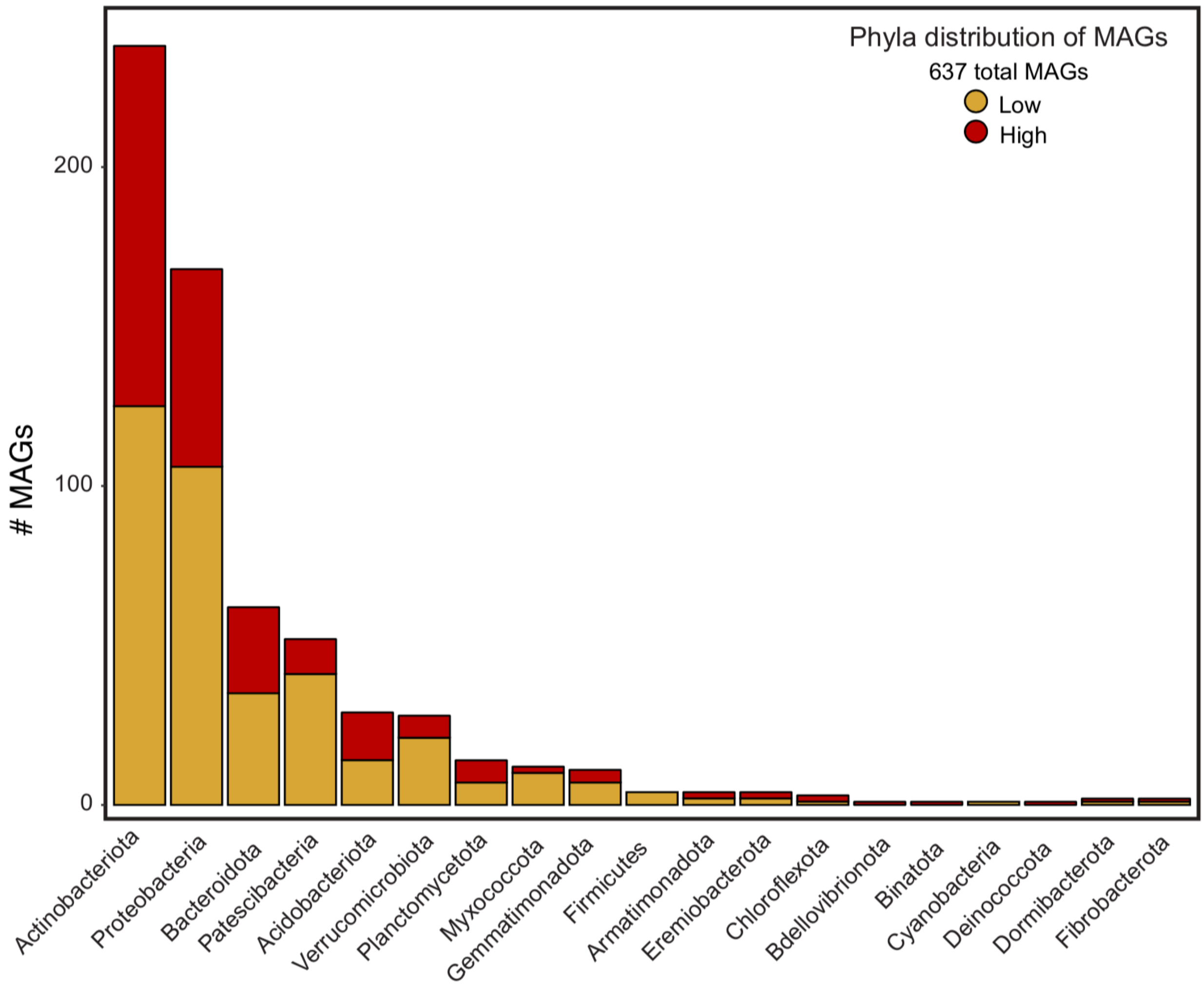

Figure S4. Phyla distribution of the 637 medium- and high-quality MAGs (> 50% completion, <10% contamination) from burned O- and A-horizon soils.

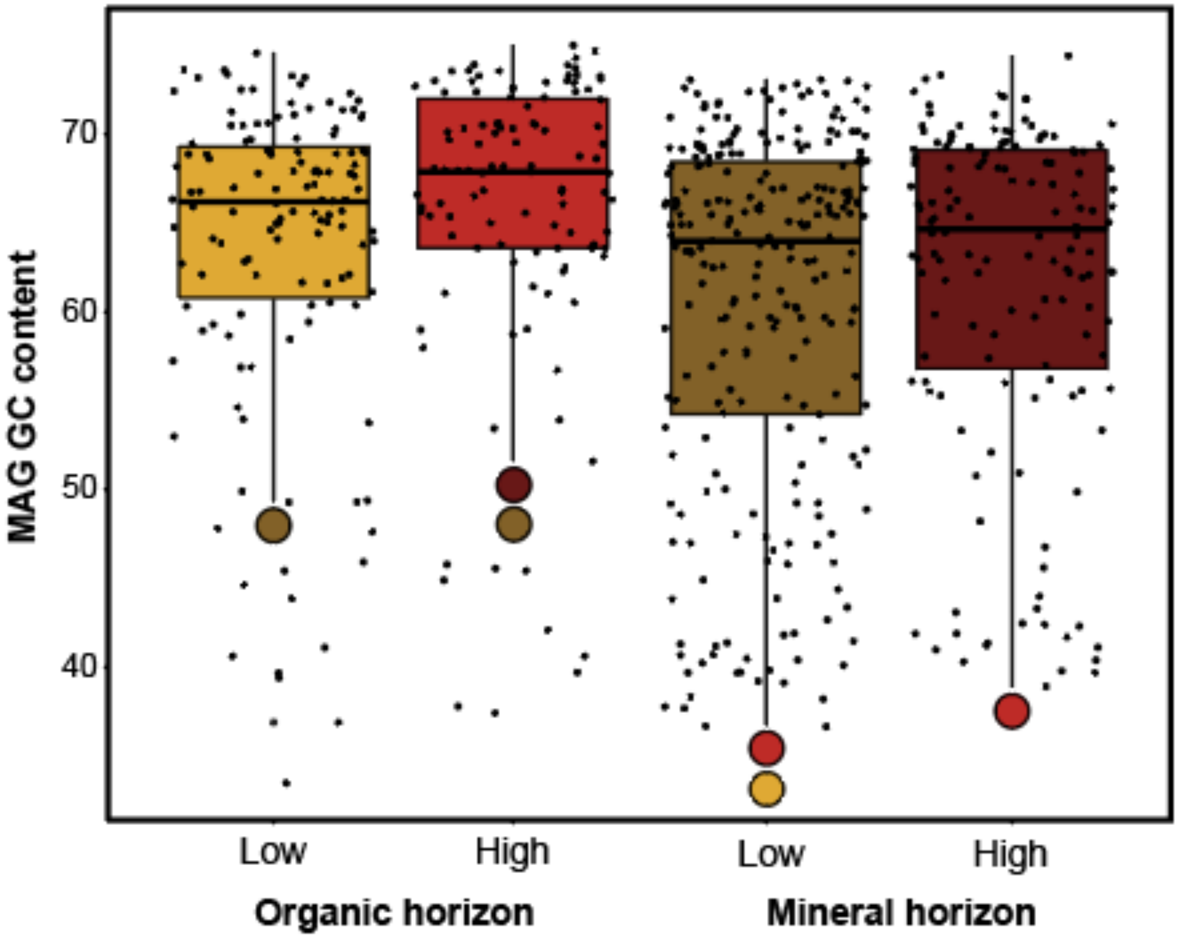

Figure S5. GC content of MAGs reconstructed from each condition. Colored points indicate significance ($p<0.05$) between conditions.

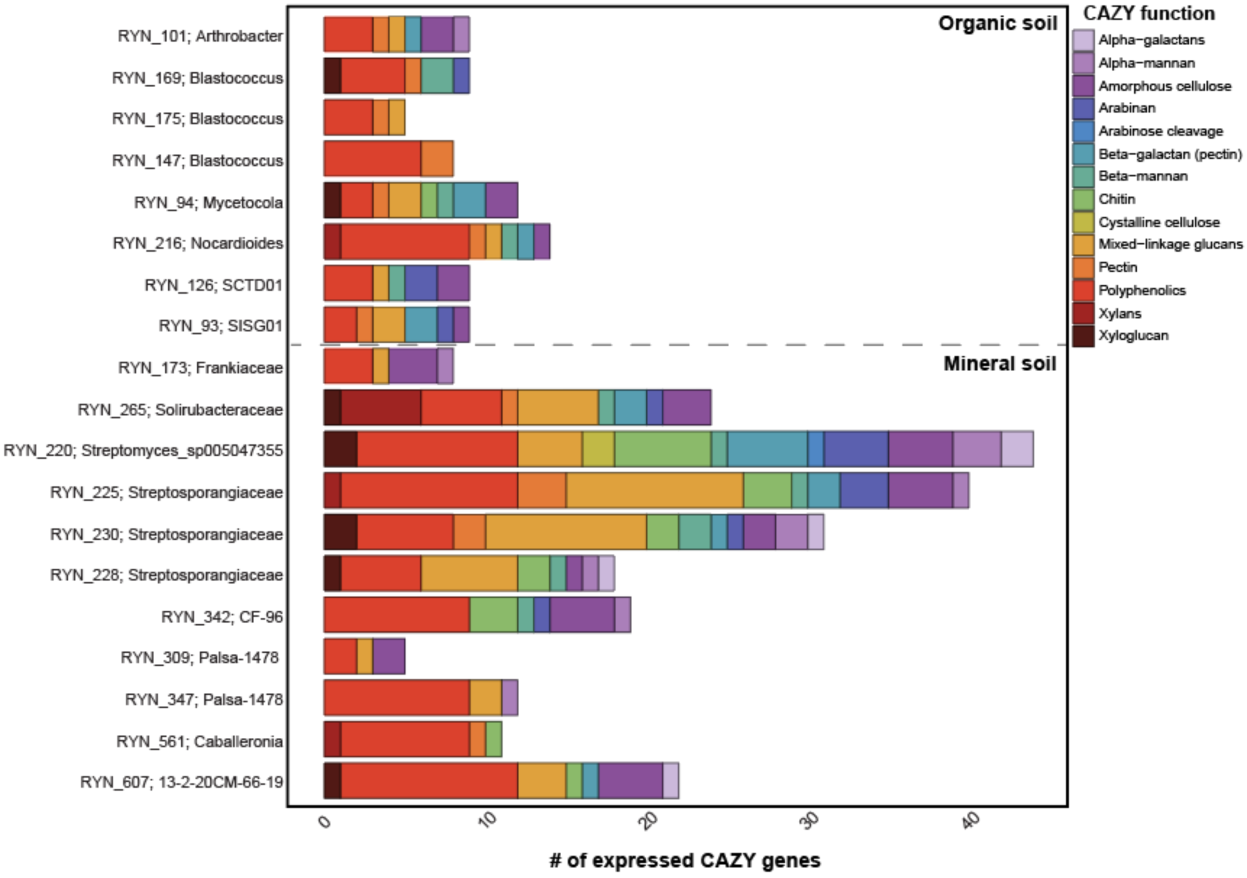

Figure S6. Functional diversity of expressed CAZYmes of the MAGs of interest from High O and High A soils.

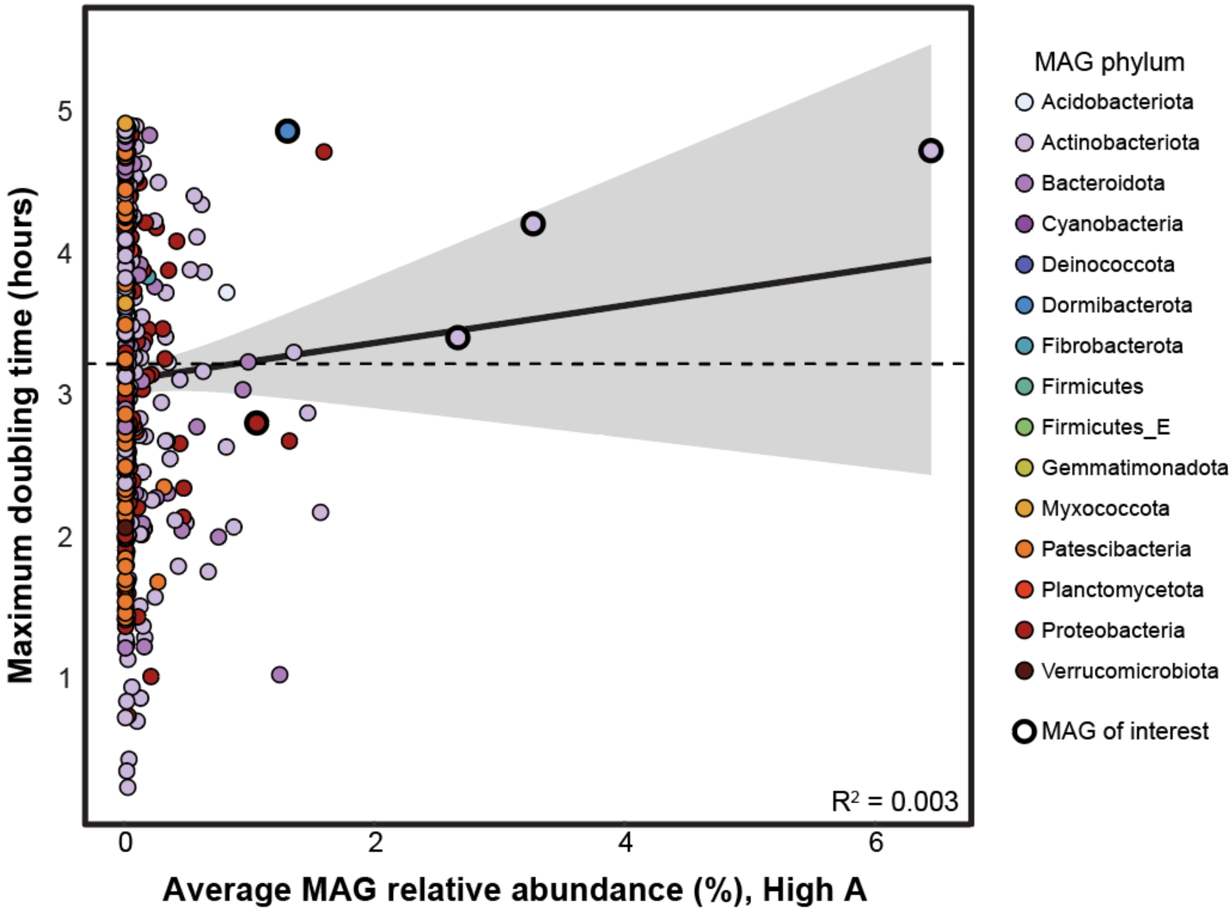

Figure S7. The average relative abundance of the MAG in High A soils plotted against maximum doubling time. MAGs of interest are bolded.

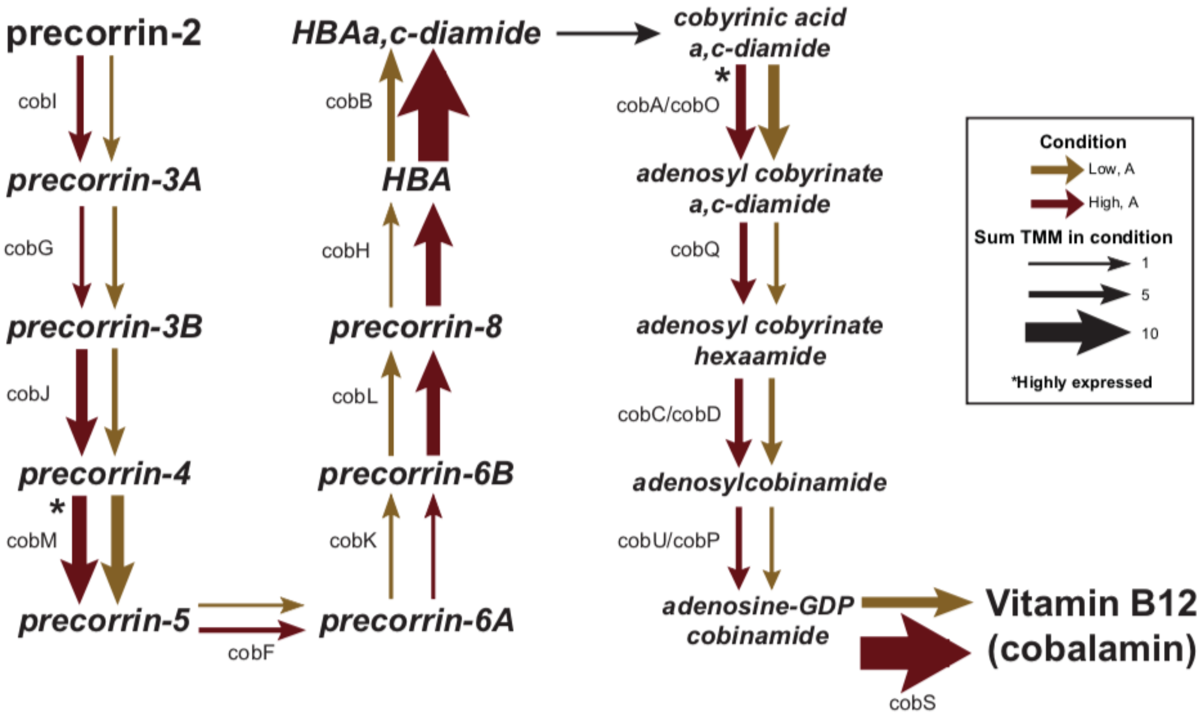

Figure S8. The aerobic cobalamin biosynthesis pathway (adapted from Doxey et al., 2015 and Lu et al., 2020) with arrows indicating the summed TMM in the colored condition.

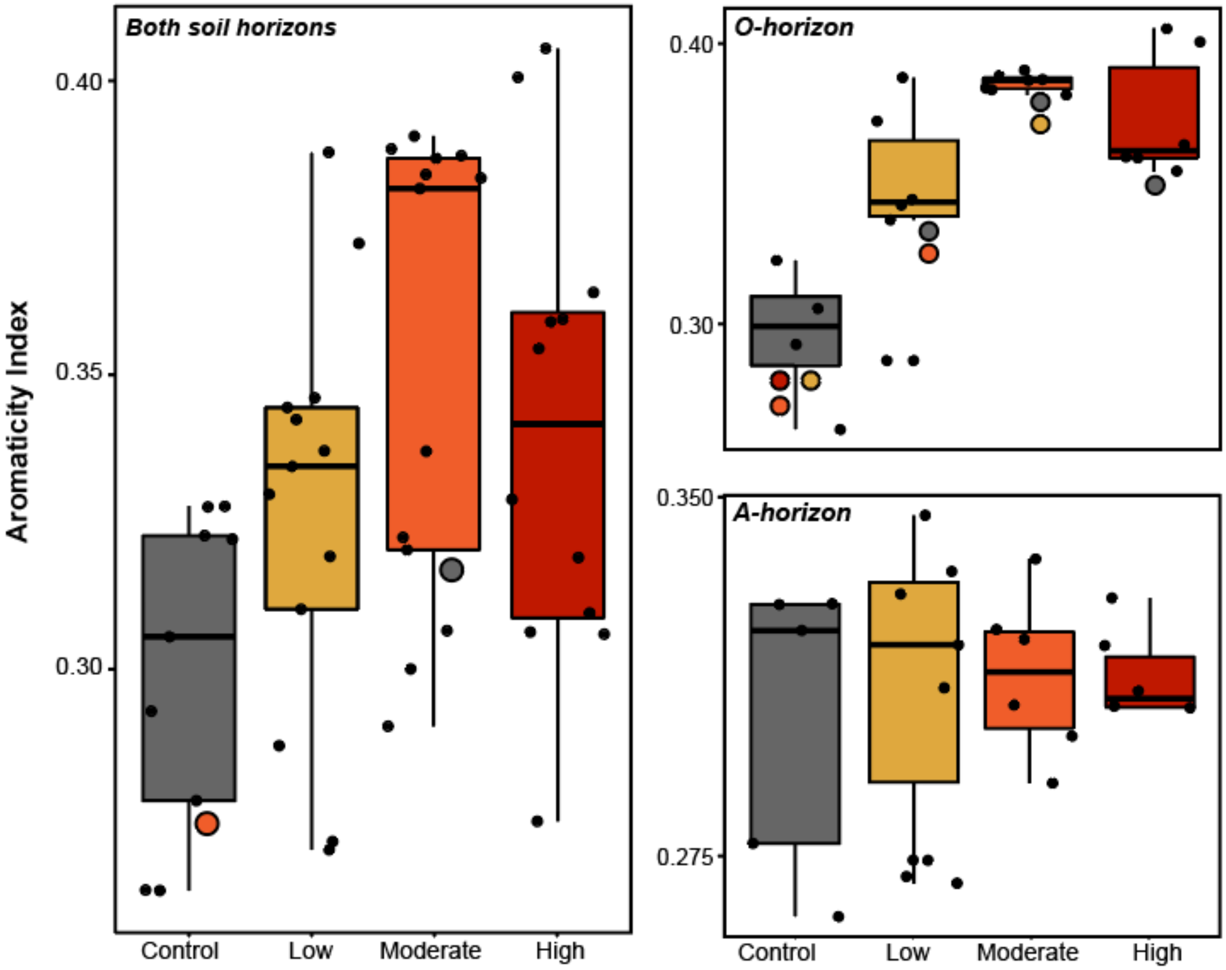

Figure S9. Aromaticity index of DOM pools against burn severity conditions and soil horizons. Colored circles indicate significance between the indicated conditions.

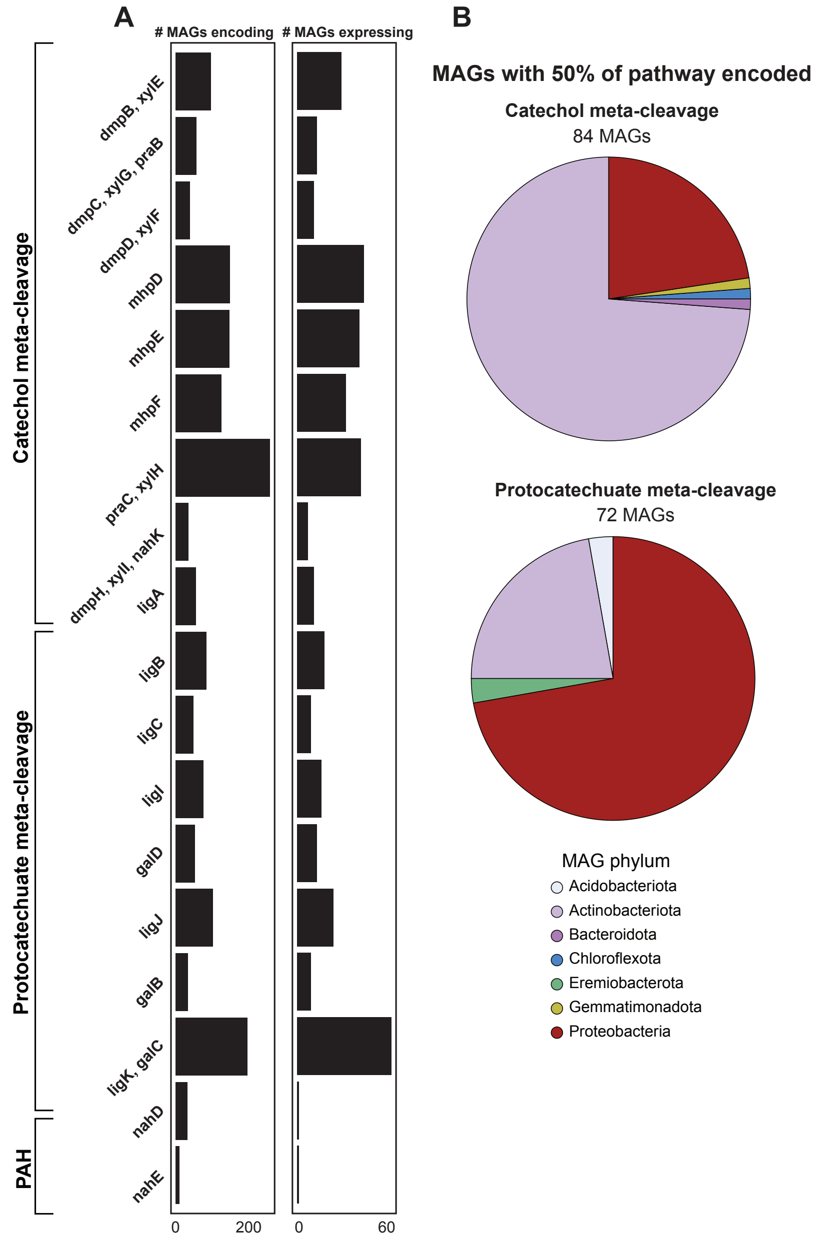

Figure S10. (A) Number of MAGs encoding and expressing each gene of the catechol and protocatechuate meta-cleavage pathways. **(B)** Phyla distribution of MAGs encoding 50% of either pathway.

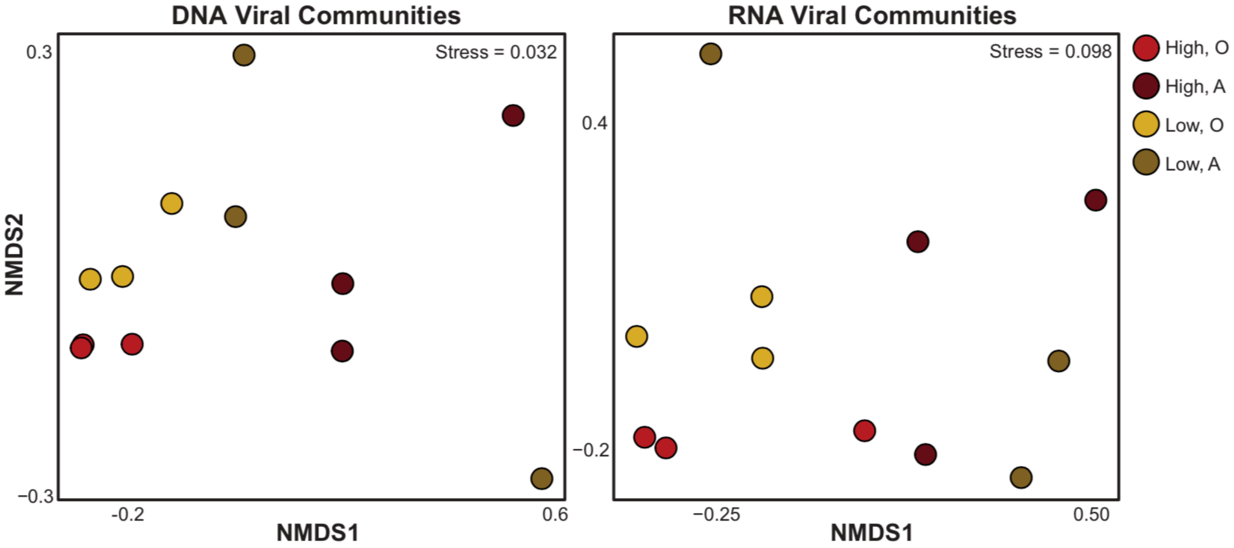

Figure S11. NMDS of DNA (left) and RNA (right) vMAG abundance across all four conditions.

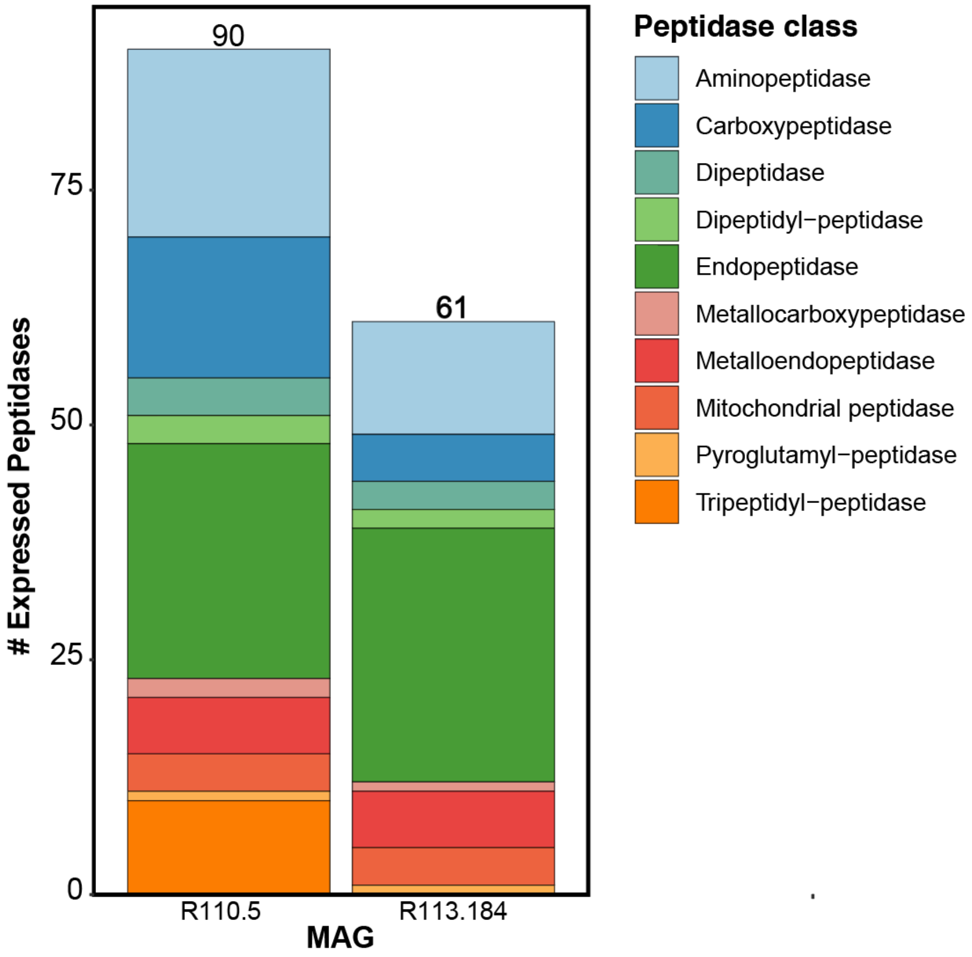

Figure S12. The diversity of peptidases expressed by each fungal MAG across all 4 conditions.

Ecological guild	# ESVs	% Change with Low	% Change with Mod	% Change with High
Arbuscular Mycorrhizal	17	-100	-96.65	-100
Ectomycorrhizal	321	-99.71	-99.93	-99.92
Endophyte	39	-94.26	-95.96	-99.91
Epiphyte	31	-81.06	-99.34	-98.78
Saprotroph	1624	228.87	260.75	281.42

Table S3. Percent change in relative abundance from control to low, moderate, and high severity in O-horizon soils of all ESVs assigned to each ecological guild by FUNguild.